



CO<sub>2</sub>  
Human  
Emissions

# Model systems and simulation configurations

J.-M. Haussaire

[che-project.eu](http://che-project.eu)



Co-ordinated by  
 ECMWF



# CO<sub>2</sub> Human Emissions

## D2.1 Model systems and simulation configurations

<b>Dissemination Level:</b>	Public
<b>Author(s):</b>	J.-M. Haussaire (Empa), D. Brunner (Empa), J. Marshall (MPG), P. Prunet (SPASCIA), A. Agustí-Panareda (ECMWF), A. Manders (TNO), A.J. Segers (TNO), H. Denier van der Gon (TNO), G. Maenhout (JRC), S. Houweling (SRON), M. Krol (SRON)
<b>Date:</b>	28/03/2018
<b>Version:</b>	2.0
<b>Contractual Delivery Date:</b>	31/03/2018
<b>Work Package/ Task:</b>	WP2/ T2.1
<b>Document Owner:</b>	Empa
<b>Contributors:</b>	TNO, ECMWF, MPG, SRON, SPASCIA, JRC
<b>Status:</b>	Final

AIRBUS





# CO<sub>2</sub> Human Emissions

## CHE: CO<sub>2</sub> Human Emissions Project

Coordination and Support Action (CSA)  
H2020-EO-3-2017 Preparation for a European  
capacity to monitor CO<sub>2</sub> anthropogenic emissions

**Project Coordinator:** Dr Gianpaolo Balsamo (ECMWF)  
**Project Start Date:** 01/10/2017  
**Project Duration:** 39 months

**Published by the CHE Consortium**

**Contact:**

ECMWF, Shinfield Park, Reading, RG2 9AX,  
[gianpaolo.balsamo@ecmwf.int](mailto:gianpaolo.balsamo@ecmwf.int)



The CHE project has received funding from the European Union's Horizon 2020 research and innovation programme under grant agreement No 776186.



## Table of Contents

1	Executive Summary .....	7
2	Introduction .....	7
2.1	Background.....	7
2.2	Scope of this deliverable .....	7
2.2.1	Objectives of this deliverable .....	7
2.2.2	Work performed in this deliverable .....	8
2.2.3	Deviations and counter measures .....	8
3	Model descriptions .....	8
3.1	CAMS CO <sub>2</sub> /IFS (ECMWF).....	8
3.2	COSMO-GHG (Empa) .....	8
3.3	LOTOS-EUROS (TNO).....	9
3.4	WRF-Chem and WRF-GHG (MPG and SRON) .....	9
3.5	EULAG (SPASCIA).....	9
4	Global simulations.....	10
4.1	Model used and its domain .....	10
4.2	Emission inventory.....	10
4.2.1	Anthropogenic emissions .....	10
4.2.2	Emission scenarios for future emissions .....	11
4.2.3	Natural emissions .....	11
4.3	Initial and boundary conditions.....	11
4.4	Model outputs .....	11
4.4.1	3D meteorology .....	12
4.4.2	2D meteorology .....	12
4.4.3	3D tracers .....	12
4.4.4	2D tracers .....	13
5	European simulations .....	13
5.1	Models used and their domain .....	13
5.1.1	Minimal domain.....	13
5.1.2	COSMO-GHG.....	13
5.1.3	LOTOS-EUROS.....	14
5.1.4	WRF-GHG .....	14
5.2	Emission inventory.....	15
5.2.1	Anthropogenic emissions .....	15
5.2.2	Emission scenarios for future emissions .....	17
5.2.3	Biogenic emissions .....	17
5.3	Initial and boundary conditions.....	17
5.3.1	Simulation strategy for the online models (COSMO-GHG and WRF-GHG)....	18

5.3.2	Specific inputs for the offline model LOTOS-EUROS .....	18
5.4	Model outputs .....	19
5.4.1	3D meteorology (COSMO-GHG and WRF-GHG) .....	19
5.4.2	2D meteorology (COSMO-GHG and WRF-GHG) .....	19
5.4.3	3D chemically passive tracers (All) .....	20
5.4.4	3D tracers for WP4 (COSMO-GHG and WRF-GHG) .....	20
5.4.5	3D chemistry (LOTOS-EUROS).....	21
5.4.6	3D aerosols (LOTOS-EUROS) .....	21
5.4.7	2D fields (All) .....	21
6	Berlin simulations.....	22
6.1	Models used and their domain .....	22
6.1.1	Minimum domain .....	22
6.1.2	COSMO-GHG.....	22
6.1.3	LOTOS-EUROS.....	23
6.1.4	WRF-CHEM.....	23
6.2	Emission inventory.....	23
6.2.1	Anthropogenic emissions.....	23
6.2.2	Biogenic emissions .....	24
6.3	Model outputs .....	24
7	Beijing simulations .....	24
7.1	Models used and their domain .....	24
7.1.1	LOTOS-EUROS.....	24
7.1.2	WRF-CHEM.....	24
7.2	Emission inventory.....	24
7.2.1	Anthropogenic emissions.....	24
7.2.2	Biogenic emissions .....	25
7.3	Model outputs .....	25
8	Power plant test case.....	25
8.1	Models used and their domain .....	25
8.1.1	COSMO-GHG.....	25
8.1.2	EULAG .....	26
8.2	Initial and boundary conditions.....	27
8.3	Model outputs .....	27
9	Conclusion.....	27
10	References.....	27
11	Annex.....	32
11.1	Time profiles applied to emissions in the European and Berlin simulations.....	32
11.2	Vertical profiles applied to emissions in the European and Berlin simulations.....	36
11.3	Schematic of the interdependence of the simulations .....	37

11.4 Summary of all the simulations .....	38
---	----

## Figures

Figure 1: Minimal European simulation domain.....	13
Figure 2: COSMO-GHG simulation domain.....	14
Figure 3: WRF-GHG simulation domain.....	15
Figure 4: Emission domains.....	15
Figure 5: Example of time profiles showing diurnal and day-of-week variability of different categories.....	17
Figure 6: Simulation strategy.....	18
Figure 7: Minimal Berlin simulation domain.....	22
Figure 8: Power plant simulation domain.....	26
Figure 9: Schematic of the interdependence of the different simulations and models.....	37

## Tables

Table 1: List of 3D meteorological outputs of the global simulation .....	12
Table 2: List of 2D meteorological outputs of the global simulation .....	12
Table 3: List of SNAP sectors .....	16
Table 4: List of 3D meteorological outputs of the European simulation .....	19
Table 5: List of 2D meteorological outputs of the European simulation .....	19
Table 6: List of output chemically passive tracers .....	20
Table 7: Allocation of source categories from the Berlin inventory to the TNO-CAMS81 inventory .....	23
Table 8: Emission temporal profiles for month in year.....	32
Table 9: Emission temporal profiles for day in week.....	33
Table 10: Emission temporal profiles for hour in day (first 12 hours) .....	34
Table 11: Emission temporal profiles for hour in day (last 12 hours) .....	35
Table 12: Vertical profiles as in Bieser et al., 2011 .....	36
Table 13: List of simulations.....	38

# 1 Executive Summary

The aim of the WP2 is ultimately to produce a library of simulations for emissions and atmospheric transport. The present report describes and documents the different simulations that will be conducted, the atmospheric transport models employed, and the different emission data sets used as input for the models. Properly documenting and agreeing among the modelling groups on the specific model and simulation setups will allow us to produce a sensible library of simulations that can be used for the inter-comparison of atmospheric transport, to produce realistic synthetic satellite observations, and to investigate the influence of aerosols on the detection of urban plumes and the influence of small scale fluctuations of power plant plumes.

## 2 Introduction

### 2.1 Background

One of the critical elements of a European contribution to a global "CO<sub>2</sub> emission monitoring system" identified in the CO<sub>2</sub> report commissioned by the European Commission (Ciais et al., 2015) is a constellation of CO<sub>2</sub> satellites with imaging capability. Between 2011 and 2015, ESA conducted a detailed Phase A/B1 assessment for the CO<sub>2</sub> imaging satellite concept CarbonSat (Bovensmann et al., 2010). In two science studies (LOGOFLUX-1, 2014; LOGOFLUX-2, 2015) supporting this assessment, it was demonstrated that such a satellite would allow observation of CO<sub>2</sub> plumes of strong localized sources such as large cities and power plants and would help constrain emissions at the regional and national scale.

However, such emission quantification faces substantial challenges due to the limited precision of the satellite measurements, systematic biases introduced by incompletely accounting for the effects of aerosols and other factors in the retrieval, the limited spatial and temporal coverage and resolution of the observations, and the difficulty in separating the signals from natural CO<sub>2</sub> fluxes from those of anthropogenic emissions.

To support the assessment of the requirements for a future space mission and the challenges introduced by the issues listed above, a library of realistic CO<sub>2</sub> simulations for present-day and future emission scenarios, from the global to the regional and point-source scale is needed.

WP2 of the CHE project aims at producing such a library of simulations mimicking reality as closely as possible, so-called nature runs. This task involves six different institutes running five different atmospheric transport models. As these models diverge in many respects, the ensemble of simulations will enable a comprehensive assessment of the influence of different model resolutions and model formulations on the representation of atmospheric CO<sub>2</sub> concentrations.

### 2.2 Scope of this deliverable

#### 2.2.1 Objectives of this deliverable

The main objectives of this report are to

- document the different models, their inputs, and the simulations
- to provide a protocol for the simulations in order to harmonize the modelling strategies as well as the inputs and outputs as far as possible in order to produce a consistent, well-documented and user-friendly library of simulations

Thorough documentation avoids misunderstandings and unnecessary divergences between the different simulations. A close co-ordination between the modelling teams is particularly important as higher resolution simulations will be driven by output from the lower resolution simulations.

## 2.2.2 Work performed in this deliverable

The library of nature runs will contain simulations of atmospheric CO<sub>2</sub> at the global, European and regional scale. The regional simulations will focus on a domain covering the city of Berlin and nearby power plants as well as on a second domain centred over the city of Beijing. On top of this, very high-resolution Large Eddy Simulations (LES) of the spatio-temporal variability of CO<sub>2</sub> in a power plant emission plume will be performed.

This document first describes the models that are used for this library of runs. Then for each simulation, the key parameters will be described, including the simulation domain and period, the grid definition, the anthropogenic and biogenic emissions, the initial and boundary conditions as well as the list of outputs. All these simulations with their parameters are summarized in the Table 13. Their inter-dependences and contributions to the different tasks of WP2 are schematized in the Figure 9.

## 2.2.3 Deviations and counter measures

An emission inventory with a resolution of 1 km x 1 km was supposed to be provided over the whole Europe as an input to the European simulations. It has been agreed by the different modelling groups that such a high resolution emission inventory was too costly and unnecessary considering the relatively coarse resolution of approximately 5 km x 5 km of the European simulations. Therefore, the native 7 km x 7 km grid from TNO will be used for the European simulations and finer resolved emission fields will be generated only for the regional simulations.

No other deviations have been encountered.

# 3 Model descriptions

## 3.1 CAMS CO<sub>2</sub> /IFS (ECMWF)

The Copernicus Atmosphere Monitoring Service (CAMS) global CO<sub>2</sub> forecasting system uses the Integrated Forecast System (IFS) Numerical Weather Prediction (NWP) model from the European Centre for Medium-Range Weather Forecasts (ECMWF, <https://www.ecmwf.int/en/forecasts/documentation-and-support/changes-ecmwf-model/ifs-documentation>) to simulate the meteorological fields and CO<sub>2</sub> atmospheric concentrations, as well as other tracers (e.g. CH<sub>4</sub> and linear CO). The transport in the IFS is based on a semi-Lagrangian advection scheme (Temperton et al., 2001; Hortal, 2002; Untch and Hortal, 2006), as well as a turbulent mixing scheme (Beljaars and Viterbo, 1998; Koehler et al., 2011; Sandu et al., 2013) and a convection scheme (Tiedtke, 1989; Bechtold et al., 2008, 2014). Because the advection scheme is not mass conserving, a mass fixer is applied to the atmospheric tracer fields (see Agustí-Panareda et al. (2017) and Diamantakis and Agustí-Panareda (2018) for further details).

## 3.2 COSMO-GHG (Empa)

The Consortium for Small-Scale Modelling (COSMO) is a consortium of seven European national weather services formed in October 1998 which aims to develop, improve and maintain a non-hydrostatic limited area atmospheric model. The COSMO model is used for both operational and research applications by the members of the consortium, universities and research institutes.

The COSMO-GHG model is an extension of COSMO with modules for the passive transport of greenhouse gases (GHG). The extension builds on the tracer module, which was developed for COSMO to provide a flexible mechanism for incorporating passively

transported tracers (Roches and Fuhrer, 2012). The tracer module has been fully integrated in COSMO version 5.0 and also in the graphics processing unit (GPU) accelerated version of the model, called COSMO-POMPA. COSMO-GHG includes additional routines for simulating a set of tracers which are not only passively transported but also experience the influence of three-dimensional emissions or surface fluxes read in from external datasets (Liu et al., 2017). For the simulations conducted here, the Smartcarb\_ser branch of the COSMO-POMPA model version 5.0\_2017.5 is used, which was developed for the ESA project SMARTCARB.

### 3.3 LOTOS-EUROS (TNO)

LOTOS-EUROS is an offline regional-scale Eulerian chemistry-transport model of intermediate complexity, developed in the Netherlands. It was originally developed for ozone and sulfur dioxide air pollution but extended to cover other gases and aerosols in a bulk approach (fine and coarse mode aerosol). Gas-phase chemistry is a condensed version of the carbon bound mechanism CBM-IV (Gery et al., 1989). For aerosols ISORROPIA II (Fountoukis and Nenes, 2007) is used. The original approach with a mixing layer and reservoir layers in the lower troposphere is modified to efficiently use the input meteorology, to increase the vertical extent, and to be able to run on a higher horizontal resolution. Anthropogenic emissions are taken from an inventory, but emissions from sea salt, mineral dust and biogenic volatile organic compounds (VOC) are calculated online. Model output consists of hourly concentration and deposition fields, as well as aerosol optical depth (AOD). Details can be found in Manders et al. (2017).

### 3.4 WRF-Chem and WRF-GHG (MPG and SRON)

The Weather Research and Forecast (WRF) NWP model, with the Advanced Research WRF (ARW) core, uses fully compressible, Euler non-hydrostatic equations on an Arakawa C-staggered grid with conservation of mass, momentum, entropy and scalars (Skamarock et al., 2008). WRF-Chem has been developed in parallel, and allows for the calculation of online chemistry. For the application to greenhouse gases, which are treated as passive tracers, the Greenhouse Gas model (WRF-GHG) was developed by Beck et al. (2011). In this case, tracers are transported online passively, i.e. without any chemical reactions, and there are optional modules for the calculation of online fluxes (such as Vegetation Photosynthesis and Respiration Model (VPRM) biospheric CO<sub>2</sub> fluxes or wetland methane fluxes) using simulated meteorological conditions as input. Since WRF-Chem version 3.5, the WRF-GHG module has been integrated directly into the WRF-Chem code, and is one of the many available chemistry options.

For the simulations performed by MPG, WRF-Chem version 3.9.1 is used. Tracer fluxes are read in as three-dimensional emission fields, which in the currently employed setup have hourly temporal resolution.

For the simulations performed by SRON, WRF-Chem version 3.8.1 is used. The interfaces to emissions and boundary conditions were developed by Super et al. (2016) and Dekker et al. (2017). The SRON implementation of CO<sub>2</sub> in WRF-Chem was developed as part of the ESA AeroCarb project.

### 3.5 EULAG (SPASCIA)

EULAG is a reference Large Eddy Simulation (LES) code for modelling turbulent dispersion in the atmospheric convective boundary layer. The EULAG model (<http://www.mmm.ucar.edu/eulag/>) is released on the public domain. EULAG is a numerical solver for all-scale geophysical flows. The underlying anelastic equations are solved either in an Eulerian (flux form) or in a Lagrangian (advective form) framework. The EULAG model is an ideal tool to perform numerical experiments in a virtual laboratory with time-dependent

adaptive meshes and within complex, and even time-dependent model geometries. These abilities are due to the unique model design that combines the nonoscillatory forward-in-time (NFT) numerical algorithms and a robust elliptic solver with generalized coordinates. The code is written as a research tool with numerous options controlling the numerical accuracy and to allow for a wide range of numerical sensitivity tests. The formulation of the model equations allow for various derivatives of the code including codes for stellar atmospheres, ocean currents, sand dune propagation or biomechanical flows.

## 4 Global simulations

Two sets of global simulations will be carried out during the project. The first ones, coined tier-1, will use currently available emission data. These first runs are required to provide on time the boundary conditions for the European and regional simulations. The tier-2 runs however will benefit from an updated version of the EDGAR emission inventory and learn from the other runs of the library. Moreover, an ensemble technique will be used to provide an uncertainty estimate. In addition, a full chemistry module might also be considered for this second set of global runs.

### 4.1 Model used and its domain

The global nature runs for CO<sub>2</sub> are performed using the Copernicus Atmosphere Monitoring Service (CAMS) CO<sub>2</sub> forecasting system (Agustí-Panareda et al., 2014, Agustí-Panareda et al., 2016, Agustí-Panareda et al., 2017). For the tier-1 simulations, the same configuration as the CAMS high resolution forecast is adopted (Diamantakis and Agustí-Panareda, 2018).

The model resolution is approximately 9 km x 9 km in the horizontal with 137 vertical levels and a time step of 7.5 minutes. The nature run extends the period from 1 January 2015 to 31 December 2015. The month of August 2012 and some additional weeks in 2013, from 11 January to 24 January and 16 June to 29 June, will possibly be simulated as well to provide boundary conditions to the Beijing and the power plant simulations.

### 4.2 Emission inventory

#### 4.2.1 Anthropogenic emissions

##### 4.2.1.1 Tier-1

The surface fluxes of CO<sub>2</sub> and CH<sub>4</sub> are all prescribed from inventories and climatologies. Anthropogenic emissions are taken from EDGAR v4.2 FT 2010 (Olivier et al., 2015) for CH<sub>4</sub> and CO<sub>2</sub> and from CAMS MACCity (Granier et al., 2011) for CO.

There is no temporal variability in these runs for CO<sub>2</sub> emissions. Anthropogenic emissions of CO, on the other hand, have a month-to-month variation and emissions of CH<sub>4</sub> have a seasonal cycle for the emissions from rice paddies. No vertical profile is used for the anthropogenic emissions.

##### 4.2.1.2 Tier-2

For the tier-2 runs, JRC will provide CO<sub>2</sub> emissions as gridded maps with 0.1° x 0.1° horizontal resolution and annual temporal resolution. They will be derived from the EDGAR v4.3.2 FT 2017 on which a fast-track approach will be applied to calculate the 2015 emissions. The CO and CH<sub>4</sub> emissions will be provided by CAMS.

JRC will also provide temporal profiles that are still to be defined. These profiles, however, may not be used for the tier-2 runs but only for lower resolution simulations run in the ensemble context.

If it is deemed necessary, the vertical profiles presented in the Section 5.2.1.4 for the European simulations will be used.

### 4.2.2 Emission scenarios for future emissions

Two emission scenarios based on the 2005 emissions will be made available based on the following assumptions:

- Business As Usual (BAU)
- Climate Change (CC) mitigation measures.

The underlying assumptions are described in the TNO-CO<sub>2</sub>\_CIRCE projections (2005-2050).

These emission scenarios will be applied to the EDGAR emission inventory used in the tier-2 runs. The simulations using these emissions will be used as boundary conditions for the European runs where the same scenarios are applied.

### 4.2.3 Natural emissions

The CO<sub>2</sub> emissions from land vegetation are modelled online using the CTESSEL Carbon module integrated in the land surface model of the IFS (Boussetta et al., 2013). The fluxes have been evaluated with FLUXNET data and compared to different models (e.g. CASA and ORCHIDEE) with a comparable performance on synoptic to seasonal scales (Balzarolo et al., 2014). An online bias correction scheme (Agustí-Panareda et al., 2016) is applied to the modelled Gross Primary Production (GPP) and ecosystem respiration (RA) fluxes to correct for biases in the net ecosystem exchange (NEE) budget compared to a climatology of optimized fluxes (Chevallier et al., 2010). Because the climate drivers of the NEE fluxes such as radiation, soil moisture and temperature might vary with the model resolution, the NEE fluxes and their budget will also vary with model resolution. This only affects CO<sub>2</sub>, as CH<sub>4</sub> and CO only have prescribed fluxes. The ocean CO<sub>2</sub> fluxes are prescribed from the Takahashi et al. (2009) climatology and fire emissions from the Global Fire Assimilation System (GFAS) (Kaiser et al., 2012). For the tier-2 runs, there is the possibility of updating the ocean fluxes from the Takahashi et al. (2009) climatology to SOCAT-based dataset (e.g. Rodenbeck et al. 2014).

The CH<sub>4</sub> fluxes and chemical sink in the simulations are based on prescribed climatologies and inventories as used by the operational IFS CAMS CH<sub>4</sub> analysis and forecast system. It uses emissions and sinks similar to Massart et al. (2014), except for the climatology of wetland emissions which has been changed from Kaplan to LPJ-HYMN dataset (Spanhi et al., 2011).

The prescribed surface fluxes for CO are described in Inness et al. (2015) and the linear chemistry scheme for CO is documented in Claeysman et al. (2010).

## 4.3 Initial and boundary conditions

The initial conditions for CO<sub>2</sub> and CH<sub>4</sub> on 1 January 2015 are extracted from the CAMS GHG analysis (Massart et al., 2014, 2016) for CO<sub>2</sub> and CH<sub>4</sub> and from the CAMS near-real time analysis (Inness et al., 2015) for CO.

The meteorology is initialized using the operational ECMWF NWP analysis. Moreover, the simulations are performed using the cyclic forecast configuration with the IFS NWP model. This means that the meteorology is re-initialised daily at 00:00 UTC using again the operational ECMWF NWP analysis, but the CO<sub>2</sub> and CH<sub>4</sub> and linear CO tracers are allowed to evolve freely, i.e. without any constraint from observations.

## 4.4 Model outputs

The list of model outputs from the global simulation is listed hereafter. These outputs are necessary for the nesting of the other simulation domains. They will be provided as 3-hourly data.

#### 4.4.1 3D meteorology

Table 1: List of 3D meteorological outputs of the global simulation

Variable name	Variable abbreviation
Specific humidity	Q
Temperature	T
Pressure	P
Wind components	U,V
Cloud liquid water content	CLWC
Cloud ice water content	CIWC

#### 4.4.2 2D meteorology

Table 2: List of 2D meteorological outputs of the global simulation

Variable name	Variable abbreviation
Geopotential and land mask	Z/LSM
Snow depth	SD
Snow temperature	TSN
Skin temperature	SKT
Skin Reservoir Content	SRC
Soil temperature	STLi
Soil wetness	SWLi
Logarithm of surface pressure	LNSP
Mean sea-level pressure	MSL
Sea-ice cover	CI
Sea surface temperature	SSTK
10 metre wind components	10U, 10V
2 metre temperature	2T
2 metre dewpoint temperature	2D

#### 4.4.3 3D tracers

- CO<sub>2</sub>
- CO
- CH<sub>4</sub>

Tagged tracers associated with different emissions (e.g. anthropogenic, biogenic, fires, oceans) are also provided by using a flux-denial configuration, where extra tracers are initialised with the realistic tracer fields with all the emissions, but are evolving without the influence of a specific type of emission during the 1-day forecast. The pattern of enhancement associated with a specific emission during the 1-day forecast can then be obtained by subtracting the full tracer with the flux-denial tracer.

#### 4.4.4 2D tracers

- XCO<sub>2</sub> [ppm]
- XCH<sub>4</sub> [ppb]
- TCCO [kg/m<sup>2</sup>].

## 5 European simulations

### 5.1 Models used and their domain

These European simulations will span the year of 2015.

#### 5.1.1 Minimal domain

All model simulations will include the following minimal domain.

- Longitude range: 11°W to 36°E
- Latitude range: 36°N to 64°N

The definition of this minimal grid allows for a better inter-comparison of results for the different modelling groups.

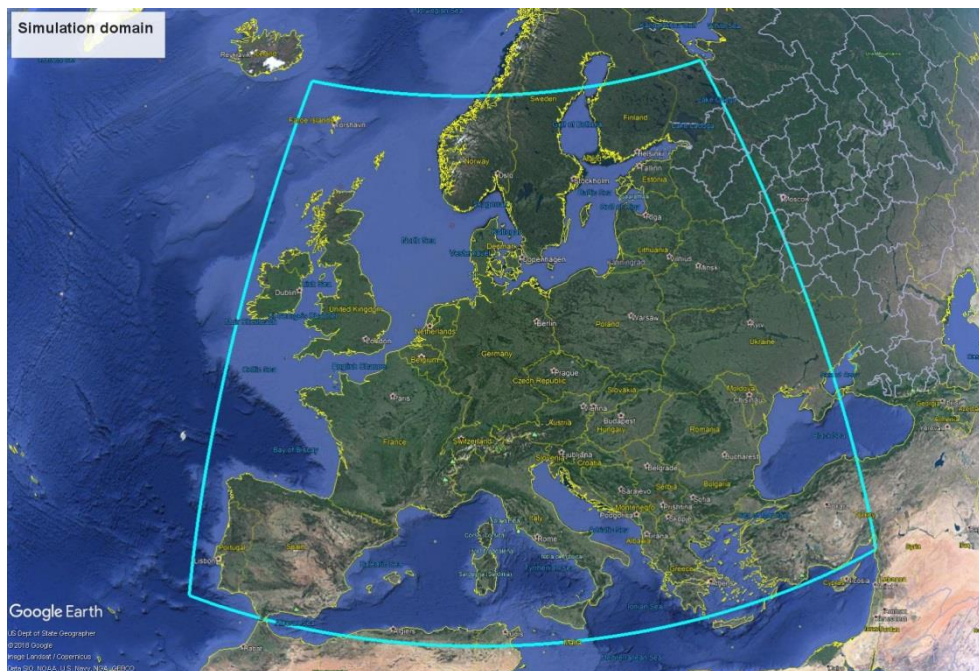


Figure 1: Minimal European simulation domain

#### 5.1.2 COSMO-GHG

COSMO-GHG uses a rotated pole projection to define its simulation grid. The domain that will be used for this simulation is as follows:

- Rotated pole: lon = -170° ; lat = 43°
- startlon = -17°
- startlat = -11°
- dlon = 0.05°
- dlat = 0.05°
- ie (nx) = 760
- je (ny) = 610

- $\text{lon}(0,0) = 10^\circ$ ,  $\text{lat}(0,0) = 47^\circ$

In the vertical, the model uses 60 layers extending from the surface to the lower stratosphere at approximately 24km.

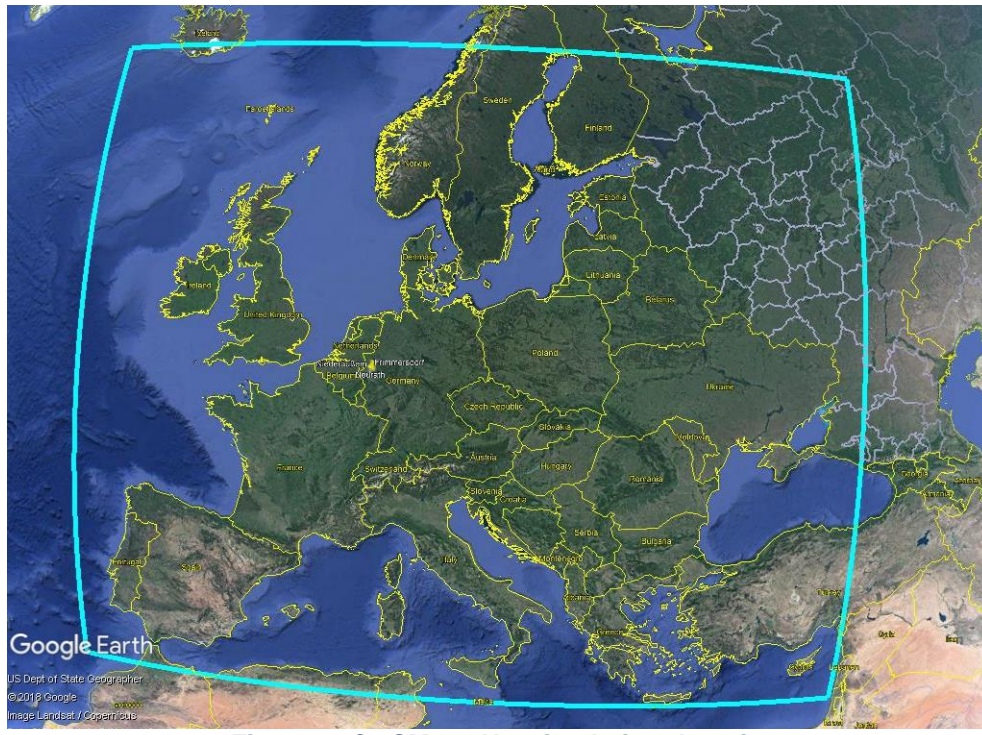


Figure 2: COSMO-GHG simulation domain

### 5.1.3 LOTOS-EUROS

This offline chemistry-transport model will be driven by hourly meteorological fields from the COSMO-GHG model above. It will thus be run on the same horizontal grid but excluding one grid cell for boundary conditions.

In the vertical, the model will cover the lower 10 km, using 12 layers based on COSMO's layer structure (lowest layer, combining next two layers, and combining each three layers going upwards).

It will produce the chemical and aerosol fields necessary for the study on the impact of aerosols on satellite XCO<sub>2</sub> performed in the task T2.4.

### 5.1.4 WRF-GHG

WRF-GHG uses a Lambert conformal projection to define its simulation grid. The domain that will be used for this simulation is as follows:

- type: Lambert conformal
- standard longitude: 12.5°
- true latitude: 51.604°
- centrepoint longitude: 12.5°
- centrepoint latitude: 51.604°
- dlon: 5 km
- dlat: 5 km
- nx: 962

- ny: 776

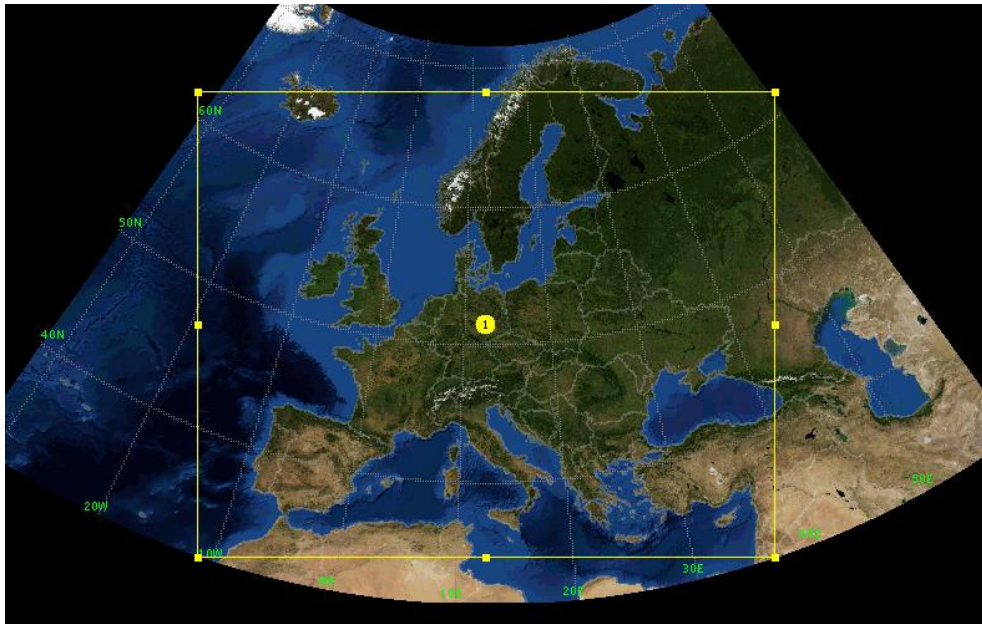


Figure 3: WRF-GHG simulation domain

## 5.2 Emission inventory

### 5.2.1 Anthropogenic emissions

The anthropogenic emissions used in the European simulations differ from the ones used in the global simulations. They are provided by TNO from the TNO-CAMS81 emissions inventory (Denier van der Gon et al., 2017), and described in this section. For comparison purposes, an extra tracer using the EDGAR emission inventory will be simulated as well (CO<sub>2</sub>\_AED in the list of outputs, see Section 5.4.3).

#### 5.2.1.1 Domain and resolution

The TNO/CAMS emission inventory covers the domain:

- Longitude range: 60°W to 60°E
- Latitude range: 30°N to 72°N

at resolution 0.125° x 0.0625° longitude-latitude (~7 km x 7 km). The domain encompasses the simulation domains of all European models.

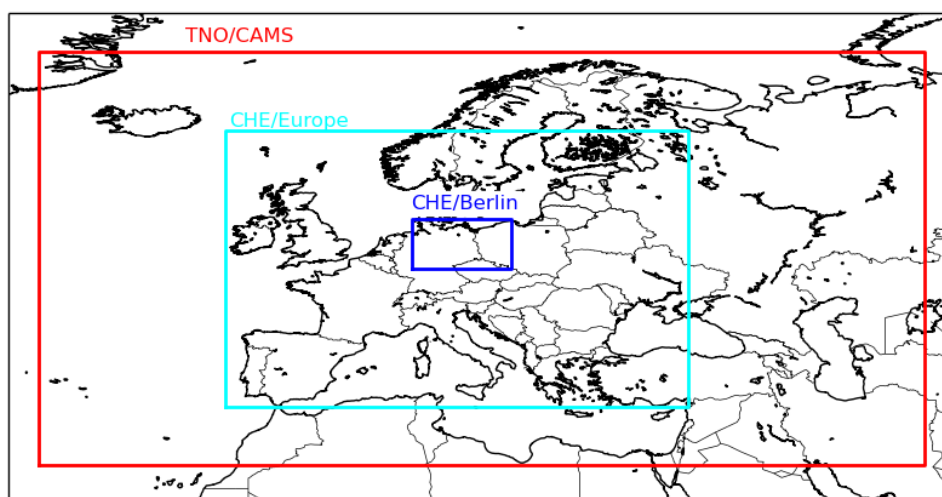


Figure 4: Emission domains

### 5.2.1.2 Sectors

Emission sectors are defined with a SNAP1 code (main category and 1 subcategory):

**Table 3: List of SNAP sectors**

<b>SNAP1</b>	<b>Emission sector</b>
01.00	Public power stations
02.00	Commercial, institutional and residential combustion
34.00	Industry
05.00	Extraction and distribution of fossil fuels
06.00	Solvents
07.01	Road transport – gasoline
07.02	Road transport – diesel
07.03	Road transport – LNG
07.04	Road transport – evaporation
07.05	Road transport – brakewear
08.00	Non-road transport
09.00	Waste treatment
10.00	Agriculture

Emissions from the two SNAP categories 03.00 and 04.00 are combined into a single category denoted as 34.00.

### 5.2.1.3 Time profiles

For the temporal distribution of the TNO/CAMS emissions, tables with metadata are provided in .csv format for all modellers to use. They are reported in Table 8, Table 9 and Table 10 in the Annex. They provide respectively the month in year, day in week and hour in day coefficients.

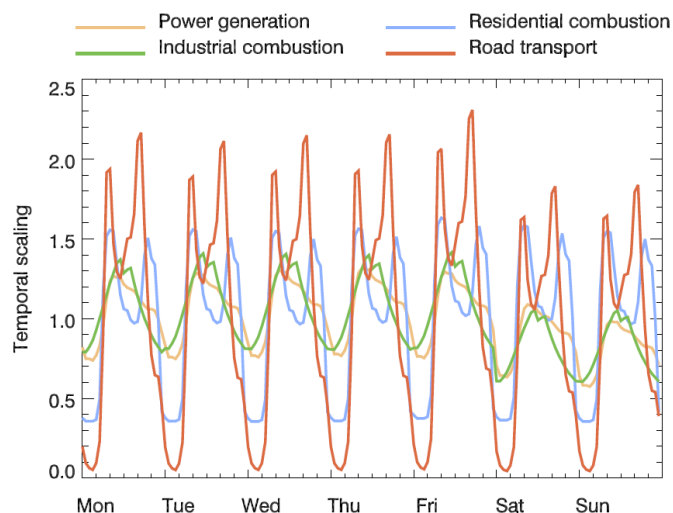


**Figure 5: Example of time profiles showing diurnal and day-of-week variability of different categories.**

#### 5.2.1.4 Vertical profiles

The height distributions for the TNO/CAMS emission inventory are defined per SNAP sector in Table 12 in the Annex. The distribution is based on Table 3 in Bieser et al., 2011, with an extra split of the lowest layer to have a surface layer of 0-20 m.

#### 5.2.2 Emission scenarios for future emissions

The same emission scenarios as the ones mentioned in Section 4.2.2 will be applied to the TNO-CAMS81 inventory.

#### 5.2.3 Biogenic emissions

Biogenic emissions, separated into gross ecosystem exchange (GPP) and respiration (RA) are provided by MPI-BGC, based on the Vegetation Photosynthesis and Respiration Model (VPRM, Mahadevan et al., 2008). These will be provided at hourly, 1-kilometer resolution on a domain containing the largest of the modelling grids used for European runs in this work package. The VPRM model is driven with indices (Enhance Vegetation Index EVI and Land Surface Water Index LSWI) which are calculated from MODIS 8-day reflectance data. In addition to this, temperature and shortwave radiation at the surface are required. The fluxes could be calculated online using meteorological data from the mesoscale model, but for CHE the fluxes will be calculated offline using output from ECMWF IFS runs at the highest spatial resolution possible. This could be provided 3-hourly by the tier-1 global runs (at ~9 km resolution) to be fully consistent, but a first version will be provided using hourly output from analysis runs already stored in the Meteorological Archival and Retrieval System (MARS) at 0.125° resolution. The model parameters have been optimized for each of seven vegetation classes based on European flux tower data from the year 2007. The land cover per grid box is estimated by the SYNMAP data product (Jung et al., 2006) at 1-km resolution. Despite the relatively coarse meteorological input, the fine structure of the fluxes is provided by the kilometeric scale of the MODIS radiances and the land cover map.

### 5.3 Initial and boundary conditions

The meteorological and chemical (CO<sub>2</sub>, CO) inputs are provided by the global simulation from this library (see Section 4).

### 5.3.1 Simulation strategy for the online models (COSMO-GHG and WRF-GHG)

Similarly to the meteorology in the global simulation, it will be reinitialized every day at 00:00 UTC after a 6 hour spin up period started from 18:00 UTC. Tracer fields are copied from one simulation to the next at the end of each day to ensure a continuous simulation of tracer fields. This procedure can be schematized as in the Figure 6.

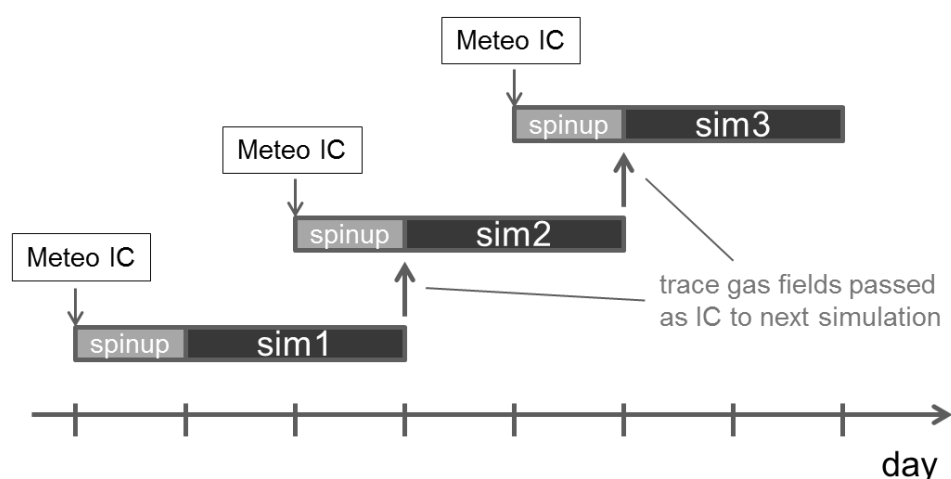


Figure 6: Simulation strategy

### 5.3.2 Specific inputs for the offline model LOTOS-EUROS

Unlike COSMO-GHG and WRF-GHG used for these European simulations, LOTOS-EUROS, as an offline model, requires meteorological data to drive its simulation. Moreover, since a full chemistry module is running, it requires specific chemical initial and boundary conditions.

#### 5.3.2.1 Meteorological fields

COSMO meteorology as delivered by Empa for this project will be used. In accordance with the output meteorological fields listed in the Sections 5.4.1 and 5.4.2, it will include:

- 3D fields:
  - T, P, U, V, Q
  - CLWC, CLC.
- 2D fields:
  - orography, land sea mask
  - boundary layer height, shortwave downward solar radiation
  - U10, V10, T2m, relative humidity at 2m (derived from Td2m), sea surface temperature
  - rain (convective + large scale), snowfall, snow depth
  - volumetric soil water (4 levels), soil type

### 5.3.2.2 Boundary condition fields for LOTOS-EUROS

As already mentioned, the global simulation will provide boundary conditions for the modelled chemical species (CO<sub>2</sub>, CO and CH<sub>4</sub>).

For other gas species and aerosols, the CAMS Reanalysis (<https://software.ecmwf.int/wiki/display/CKB/CAMS+Reanalysis+data+documentation>) should be completed in 2018 and be used to provide boundary conditions. Moreover, the tier-2 global simulations may include a full chemistry module and thus may be used instead. Alternatively, the CAMS NRT analysis could be used.

For tracers that are not available from those analyses, for example short lived tracers or lumped hydrocarbons, constant background concentrations are used.

## 5.4 Model outputs

The list of model outputs from the European simulations is listed hereafter. These outputs are necessary for the nesting of the Berlin simulation domain. They will be provided as hourly data on the native model grids.

### 5.4.1 3D meteorology (COSMO-GHG and WRF-GHG)

Table 4: List of 3D meteorological outputs of the European simulation

Variable name	Variable abbreviation
Specific humidity	Q
Temperature	T
Pressure	P
Wind components	U,V
Cloud liquid water content	CLWC
Cloud ice water content	CIWC
Cloud cover	CLC

### 5.4.2 2D meteorology (COSMO-GHG and WRF-GHG)

Table 5: List of 2D meteorological outputs of the European simulation

- Cloud and precipitation: convective and large-scale precipitation, total cloud cover, cloud optical thickness
- Diagnosed planetary boundary layer height, soil moisture (multiple layers), snow depth
- Radiation: short- and long-wave radiation at ground, all components (up- and down) separately
- Surface fluxes: Sensible and latent heat fluxes
- T and Td at 2 m, U and V at 10 m

### 5.4.3 3D chemically passive tracers (All)

Table 6: List of output chemically passive tracers

Name	Description
CO2_A	CO <sub>2</sub> using TNO emissions
CO_A	CO using TNO emissions
CH4_A	CH <sub>4</sub> using TNO emissions
CO2_AED	CO <sub>2</sub> using EDGAR emissions as in the global simulation (COSMO-GHG)
CO2_BG	CO <sub>2</sub> from boundary condition
CO_BG	CO from boundary condition
CH4_BG	CH <sub>4</sub> from boundary condition
CO2_GPP	CO <sub>2</sub> from vegetation: Gross Photosynthetic Production (GPP)
CO2_RA	CO <sub>2</sub> from vegetation: Respiration (RA)
CO2_A1	CO <sub>2</sub> using emissions from TNO for public power stations (SNAP 01.00)
CO_A1	CO using emissions from TNO for public power stations (SNAP 01.00)
CO2_A2	CO <sub>2</sub> using emissions from TNO for commercial, institutional and residential combustion (SNAP 02.00)
CO_A2	CO using emissions from TNO for commercial, institutional and residential combustion (SNAP 02.00)
CO2_A34	CO <sub>2</sub> using emissions from TNO for industry (SNAP 34.00)
CO_A34	CO using emissions from TNO for industry (SNAP 34.00)
CO2_A7	CO <sub>2</sub> using emissions from TNO for road transport (sum of SNAP 07.01-07.05)
CO_A7	CO using emissions from TNO for road transport (sum of SNAP 07.01-07.05)
CO2_AO	CO <sub>2</sub> using emissions from TNO for others (SNAP 05.00+06.00+08.00+09.00+10.00)
CO_AO	CO using emissions from TNO for others (SNAP 05.00+06.00+08.00+09.00+10.00)

### 5.4.4 3D tracers for WP4 (COSMO-GHG and WRF-GHG)

Though the scope of the present deliverable is only the library of nature runs from WP2, there are similarities between some simulations and case studies of WP2 and WP4. Consequently, the WP4 could benefit from the work in this work package. As far as possible,

if any simulation from WP2 can be reused in WP4, it ought to be. Therefore a couple of extra tracers will be added by the modelling groups who also take part in the WP4.

- CO\_R: CO with idealized decay and production (COSMO-GHG only)
- APO
- <sup>14</sup>C

Emission fields for APO and radiocarbon will be generated in WP4.

### 5.4.5 3D chemistry (LOTOS-EUROS)

LOTOS-EUROS including a full chemistry module, it will produce 3D output fields for several trace gases. These fields, combined with the aerosols, are necessary for the study of the impact of aerosols on satellite retrievals.

- O<sub>3</sub>
- NO<sub>2</sub>
- NO
- NH<sub>3</sub>
- SO<sub>2</sub>
- HNO<sub>3</sub>
- CO
- N<sub>2</sub>O<sub>5</sub>
- HCHO
- Isoprene
- PAN
- NMVOC (Total non-methane volatile organic compounds)

### 5.4.6 3D aerosols (LOTOS-EUROS)

Fine mode (PM<sub>2.5</sub>):

- sea salt
- dust
- Elemental carbon (EC)
- Primary particulate matter (PPM)
- Primary organic matter (POM)
- SO<sub>4</sub>
- NO<sub>3</sub>
- NH<sub>4</sub>

Coarse mode (2.5-10 μm):

- sea salt
- dust
- Elemental carbon (EC)
- Primary particulate matter (PPM)
- Primary organic matter (POM)
- SO<sub>4</sub>
- NO<sub>3</sub>

Aerosol optical depth (AOD) at 550 nm and 870 nm.

### 5.4.7 2D fields (All)

XCO<sub>2</sub>, XCH<sub>4</sub> and TC for all simulated 3D tracers.

## 6 Berlin simulations

These high-resolution simulations focus on a domain around the city of Berlin and the nearby power plants.

### 6.1 Models used and their domain

This Berlin case study will span the whole year 2015 for the models COSMO-GHG, but only the periods from 1 February 2015 to 20 February 2015 and from 26 June to 14 July 2015 for WRF-CHEM and LOTOS-EUROS.

#### 6.1.1 Minimum domain

All model simulations will include the following minimal domain.

- Longitude range: 8°W to 18°E
- Latitude range: 50°N to 55°N

The definition of this minimal grid allows for a better inter-comparison of results for the different modelling groups.

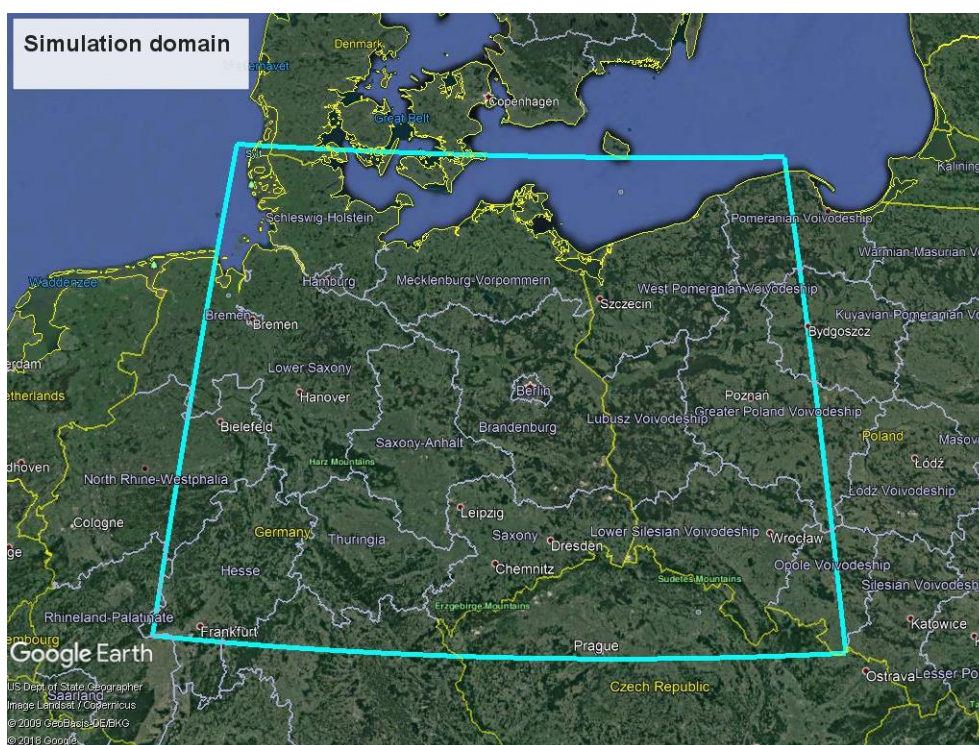


Figure 7: Minimal Berlin simulation domain

#### 6.1.2 COSMO-GHG

COSMO-GHG uses a rotated pole projection to define its simulation grid, whose pole is the same as for the European simulation. The size of the COSMO model domain is specified as 700 × 600 grid cells with a resolution of 0.01° (~1.1 km) and 60 vertical levels. The size of the domain is thus 780 km × 670 km.

- Rotated pole: lon = -170° ; lat = 43°
- startlon = -1.4°

- startlat = 2.5°
- dlon = 0.01°
- dlat = 0.01°
- ie (nx) = 700
- je (ny) = 600
- lon(0,0) = 10°, lat(0,0) = 47°

### 6.1.3 LOTOS-EUROS

Runs will be performed on the coarsened COSMO grid as described above, combining 2 COSMO cells in longitude and in latitude direction to arrive at a resolution of 0.02° (~2.2 km). One grid cell is used to accommodate the boundary conditions.

In the vertical, the lower 10 km will be covered, using the lowest layer of COSMO, combining the next two COSMO layers, and subsequently combining each three COSMO layers.

COSMO meteorology as delivered by Empa in this project will be used.

### 6.1.4 WRF-CHEM

The runs will use 4 nested domains with respective resolutions: 36, 12, 4, and 1.3 km. Domains 1 and 2 cover sizeable fractions of Western Europe. Domain 3 covers an area of 412 km x 484 km centred over Berlin. Domain 4 covers a region of 113 km x 113 km centred over Berlin. The WRF-CHEM simulations use a conical projection. The vertical resolution is 39 layers from the surface to 50 hPa.

## 6.2 Emission inventory

### 6.2.1 Anthropogenic emissions

The TNO-CAMS81 emission inventory, downscaled from its 7 km x 7 km resolution to a 1 km x 1 km resolution will be used. The domain of this high-resolution inventory will cover the minimal domain defined for this task, i.e. [8°E,18°E] x [50°N,55°N]. The planned resolution is 1/120 degree longitude x 1/60 degree latitude which is about 1 km for the chosen domain. The raster of this resolution coincides with other geographical data such as land use maps, which are often defined in arc minutes (1/60 degree) or 30 arc seconds (1/120 degree).

For the city of Berlin, an inventory with very high spatial resolution was obtained from the “Senatsverwaltung für Stadtentwicklung und Umwelt” for 2012 (Senatsverwaltung für Stadtentwicklung und Umwelt, June 2016). The inventory will be merged with the TNO-CAMS81 inventory as done previously in the ESA project SMARTCARB (Kuhlmann and Brunner, 2017). The inventory includes emissions of over 30 pollutants including CO, CO<sub>2</sub> and NO<sub>x</sub> for seven major source categories.

The major emission categories differ in the TNO-CAMS81 and Berlin inventory, but are ultimately based on NFR09 sector codes. It is hence possible to allocate the source categories from the Berlin inventory to the TNO-CAMS81 sectors.

**Table 7: Allocation of source categories from the Berlin inventory to the TNO-CAMS81 inventory**

<b>TNO-CAMS81 (SNAP1 category)</b>	<b>Berlin emission inventory (code)</b>
Public power stations (01.00)	Industry and commerce (1)

	(only the power plants)
Commercial, institutional and residential combustion (02.00)	Building heating (2)
Industry (34.00)	Industry and commerce (1) (except power plants)
Road transport (07.01-05)	Road transport <sup>1</sup> (9)
Others (05.00+06.00+08.00+09.00+10.00)	Other traffic (3) Offroad (4) Construction sites (5) Additional sources <sup>2</sup> (6) Biogenic sources <sup>3</sup> (7)

<sup>1</sup>emissions from road transport on minor roads were estimated from an inventory from 2009;  
<sup>2</sup>source category without CO, CO<sub>2</sub> or NO<sub>x</sub> emissions; <sup>3</sup>only NO<sub>x</sub> emissions will be used

The same vertical and temporal profiles as used in the European simulation will be applied (see Section 5.2.1).

### 6.2.2 Biogenic emissions

The same data set of biogenic emissions as in the European simulations will be used for the Berlin domain (see Section 5.2.2).

### 6.3 Model outputs

With the exception of the tracer CO<sub>2</sub>\_AED, and the tracers specific to the WP4, the same model outputs as in the European simulations will be generated (see Section 5.4).

## 7 Beijing simulations

These simulations focus on a domain centred over the city of Beijing. In comparison with the Berlin test case, this will allow generation of simulations for a region with different challenges in terms of emission density, interferences from aerosols, and availability and quality of input data and ground-based observations.

Simulations for Beijing will be conducted in the context of task 2.4 and are scheduled for 2019. Details on the configuration will be decided on early 2018. We report the parameters envisioned as of today.

### 7.1 Models used and their domain

#### 7.1.1 LOTOS-EUROS

The planned resolution is 3 km x 3 km.

#### 7.1.2 WRF-CHEM

The planned resolution is 4 km x 4 km.

### 7.2 Emission inventory

#### 7.2.1 Anthropogenic emissions

The EDGAR v.4.3 FT may be used.

## 7.2.2 Biogenic emissions

The same data set of biogenic emissions as in the European simulations may be used for the Beijing test case (see Section 5.2.2). If so, they will be provided at hourly resolution on the spatial grid of the WRF-CHEM model. If the LOTOS-EUROS model covers a larger domain, this would need to be adjusted.

## 7.3 Model outputs

The outputs of the model are expected to be similar to those of the Berlin test case (see Section 6.3).

# 8 Power plant test case

Note that this description could evolve or could change, depending on the priority choices which will be made in the course of the project. Alternative and complementary choices could be:

- to run a power plant simulations with both COSMO and EULAG over a Berlin case site as a preliminary test case ;
- to choose an alternative case study location and period, in place of the anticipated C-MAPEX described below, if access to a more recent and preferable campaign dataset is possible.

## 8.1 Models used and their domain

For the time being, the month of August 2012 has been chosen in order to be able to compare simulated concentrations with the C-MAPEX measurement campaign (Krings et al., 2018).

The domain will hence focus around the power plants of Niederaussem, Neurath and Frimmersdorf, near Düsseldorf. Niederaussem is the largest power plant in Germany and among the largest power plants worldwide.

### 8.1.1 COSMO-GHG

The domain that will be used for this simulation will differ from the one used in the Berlin case study to include the power plants measured in C-MAPEX.

COSMO-GHG uses a rotated pole projection to define its simulation grid. The grid will be as follows:

- Rotated pole: lon = -170 ; lat = 43
- startlon = -3.5
- startlat = 2.5
- dlon = 0.01
- dlat = 0.01
- ie (nx) = 300
- je (ny) = 300
- lon(0,0) = 10, lat(0,0) = 47

In the vertical, the model uses 60 layers, the highest one reaching the stratosphere at approximately 24 km.

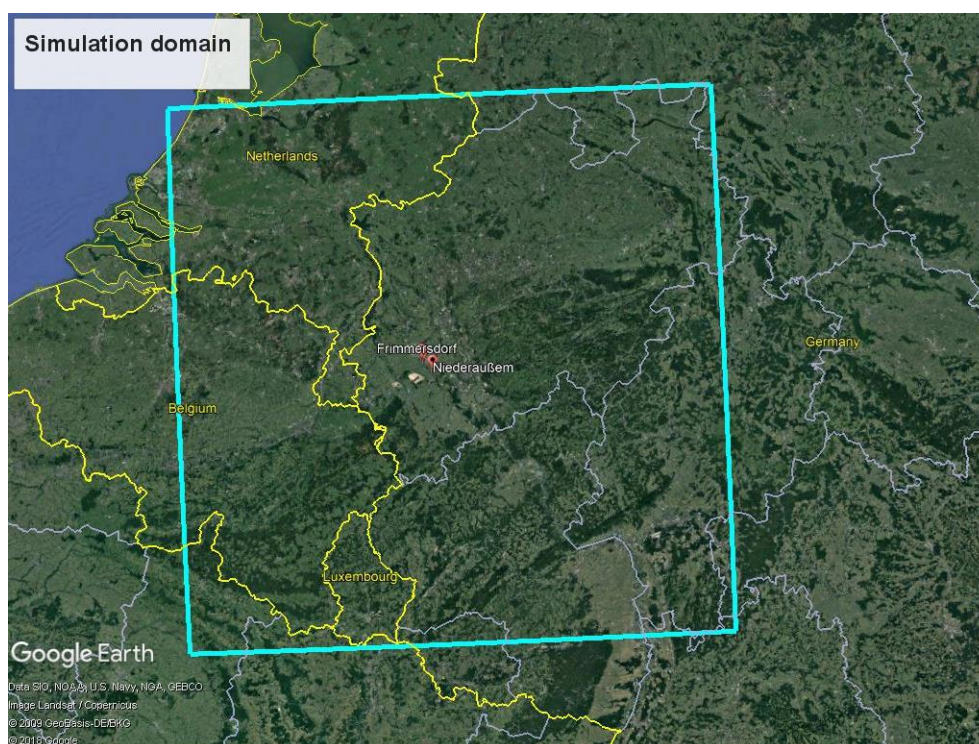


**Figure 8: Power plant simulation domain**

This run will provide meteorological data, in particular vertical profiles of wind and temperature at the location of the power plants, to constrain the EULAG model.

### 8.1.2 EULAG

At this stage, an example of a set-up of the EULAG simulation is described. This will be consolidated when more detailed information on the simulations is available.

The Boussinesq approximation is used to derive the filtered Navier-Stokes equations for the LES model. The subfilter-scale fluxes are modelled through an eddy-diffusivity. The eddy-diffusivity coefficient are calculated as a function of the subfilter-scale turbulent kinetic energy (TKE) for which a prognostic equation is solved.

At the surface, the Monin-Obukhov similarity theory is applied to calculate the surface momentum and scalar fluxes and surface scalar values.

The topographic features are modelled using the regular terrain-following coordinate transformation (used in most mesoscale model) or using the immersed boundary method in which fictitious body forces are introduced in the motion equations.

The EULAG's underlying numerics are the nonoscillatory forward-in-time scheme based on the finite difference MPDATA transport algorithm.

The large-eddy simulations will be run on a domain size corresponding to a few grid cells of a meso-scale model. Typically, the atmospheric flow contained in a volume of 40 km×20 km×1500 m can be simulated by LES by means of 400×200×60 grid points. The horizontal spatial resolution is then 100 m. The exact position and characteristics of the grid will be defined later.

The LES simulations will typically run for 3 h, with a maximum time-step used in the calculations of 1s. The first hour of simulation is devoted to the generation of meteorology dynamic. The tracers will then be released continuously from the second to the third hour.

It is possible to consider also warm source, i.e., the temperature of the source is assumed to be warmer (instead of equal) to the ambient temperature.

## 8.2 Initial and boundary conditions

The boundary conditions assumed for the dynamic and for the tracers shall be discussed and defined.

In addition, following inputs shall be defined consistently with COSMO simulation:

- the surface sensible heat flux ( $\text{Km.s}^{-1}$ );
- the initial (or timely-dependent) potential temperature profile(s) (K);
- the surface roughness length  $z_0$  (m);
- the horizontal position of the tracer release (centre of the horizontal domain ?) and the height of the tracer release;
- the emission rate of the tracer ( $\text{kg.s}^{-1}$ , the rate will be maintained constant during the simulation);
- the prescription of geostrophic wind speed ( $\text{m.s}^{-1}$ );
- the surface topographic scenario.

## 8.3 Model outputs

At the end of the EULAG simulation 4D outputs include instantaneous fields (typically each 30 seconds) of wind, potential temperature and tracer concentrations for the last 2 hours of simulation.

The outputs of the COSMO model will similar to those listed at the Section 6.3, with fewer tracers.

# 9 Conclusion

This document compiles the configuration of the various simulations that are to be part of the library of runs produced in the WP2 of the CHE project. For each of the models used in this project, a short description is provided. Moreover, for every simulation from the global to the regional scale, the temporal and spatial definition of the domain, the choice of emission inventory and parametrisation, the initial and boundary conditions as well as the selected outputs are clearly defined. This resulted from agreements amongst the different modelling groups involved in this WP.

This deliverable will serve as a reference for future work within this WP. As it provides the list of key parameters for the simulations, it should avoid any misunderstanding and divergence among modellers in the future. It has already allowed connections with WP4, which could potentially benefit from the setup of the European simulations for its inversions (to be determined). To that end, some supplementary tracers have been specifically added to the list of outputs and will be used in WP4. Moreover, for other WPs within CHE as well as for any end user of the library of runs, this document will serve as a source of metadata regarding the content of the simulations.

# 10 References

Agustí-Panareda, A., S. Massart, F. Chevallier, S. Boussetta, G. Balsamo, A. Beljaars, P. Ciais, N.M. Deutscher, R. Engelen, L. Jones, R. Kivi, J.-D. Paris, V.-H. Peuch, V. Sherlock, A. T. Vermeulen, P.O. Wennberg, and D. Wunch: Forecasting global atmospheric CO<sub>2</sub>, *Atmos. Chem. Phys.*, 14, 11959–11983, 2014.

Agustí-Panareda, A., S. Massart, F. Chevallier, G. Balsamo, S. Boussetta, E. Dutra, A. Beljaars: A biogenic CO<sub>2</sub> flux adjustment scheme for the mitigation of large-scale biases in global atmospheric CO<sub>2</sub> analyses and forecasts, *Atmos. Chem. Phys.*, 16, 10399–10418, 2016.

Agustí-Panareda, A., M. Diamantakis, V. Bayona, F. Klappenbach, and A. Butz: Improving the inter-hemispheric gradient of total column atmospheric CO<sub>2</sub> and CH<sub>4</sub> in simulations with the ECMWF semi-Lagrangian atmospheric global model, *Geosci. Model Dev.*, 10, 1–18, 2017.

Balzarolo, M., Boussetta, S., Balsamo, G., Beljaars, A., Maignan, F., Calvet, J.-C., Lafont, S., Barbu, A., Poulter, B., Chevallier, F., Szczypta, C., and Papale, D.: Evaluating the potential of large-scale simulations to predict carbon fluxes of terrestrial ecosystems over a European Eddy Covariance network, *Biogeosciences*, 11, 2661–2678, doi:10.5194/bg-11-2661-2014, 2014.

Bechtold, P., Köhler, M., Jung, T., Doblas-Reyes, F., Leutbecher, M., Rodwell, M., Vitart, F., and Balsamo, G.: Advances in simulating atmospheric variability with the ECMWF model: From synoptic to decadal time-scales, *Q. J. Roy. Meteor. Soc.*, 134, 1337–1351, 2008.

Bechtold, P., Semane, N., Lopez, P., Chaboureau, J.-P., Beljaars, A., and Bormann: Representing equilibrium and nonequilibrium convection in large-scale models, *J. Atmos. Sci.*, 71, 734–753, 2014.

Beck, V., T. Koch, R. Kretschmer, J. Marshall, R. Ahmadov, C. Gerbig, D. Pillai, and M. Heimann, (2011): The WRF Greenhouse Gas Model (WRF-GHG). Technical Report No. 25, Max Planck Institute for Biogeochemistry, Jena, Germany.

Beljaars, A. and Viterbo, P.: The role of the boundary layer in a numerical weather prediction model, in: *Clear and cloudy boundary layers*, Royal Netherlands Academy of Arts and Sciences, North Holland Publishers, Amsterdam, 1998.

Bergamaschi, P., Frankenberg, C., Meirink, J. F., Krol, M., Villani, M. G., Houweling, S., Dentener, F., Dlugokencky, E. J., Miller, J. B., Gatti, L. V., Engel, A., and Levin: Inverse modeling of global and regional CH<sub>4</sub> emissions using SCIAMACHY satellite retrievals, *J. Geophys. Res.*, 114, D22301, doi: 10.1029/2009JD012287, 2009.

Bieser, J., Aulinger, A., Matthias, V., Quante, M., & van Der Gon, H. D. (2011). Vertical emission profiles for Europe based on plume rise calculations. *Environmental Pollution*, 159(10), 2935-2946, doi:10.1016/j.envpol.2011.04.030.

Boussetta, S., Balsamo, G., Beljaars, A., Agustí-Panareda, A., Calvet, J.-C., Jacobs, C., van den Hurk, B., Viterbo, P., Lafont, S., Dutra, E., Jarlan, L., Balzarolo, M., Papale, D., and van der Werf, G.: Natural carbon dioxide exchanges in the ECMWF Integrated Forecasting System: implementation and offline validation, *J. Geophys. Res.-Atmos.*, 118, 1–24, doi:10.1002/jgrd.50488, 2013.

Bovensmann, H., Buchwitz, M., Burrows, J. P., Reuter, M., Krings, T., Gerilowski, K., Schneising, O., Heymann, J., Tretner, A., and Erzinger, J.: A remote sensing technique for global monitoring of power plant CO<sub>2</sub> emissions from space and related applications, *Atmos. Meas. Tech.*, 3, 781-811, doi: 10.5194/amt-3-781-2010, 2010.

Builtjes, P., van Loon, M., Schaap, M., Teeuwisse, S., Visschedijk, A., and Bloos, J.: Project on the modelling and verification of ozone reduction strategies: contribution of TNO-MEP, TNO-report, MEP-R2003/166, Apeldoorn, The Netherlands, 2003.

Chevallier, F. P. Ciais, T.J. Conway, T. Aalto, b.E. Anderson, P. Bousquet, E.G. Brunke, L. Ciattaglia, Y. Esaki, M. Frohlich, A. Gomez, A.J. Gomez-Peaez, L. Haszpra, P.B. Krummel, R. L. Langenfelds, M. Leuenberger, T. Machida, F. Maignan, H. Matsueda, J.A. Morgui, H. Mukai, T. Nakazawa, P. Peylin, M. Ramonet, L. Rivier, Y. Sawa, M. Schmidt, L.P. Steele, S.A. Vay, A.T. Vermeulen, S. Wofsy, D. Worthy: CO<sub>2</sub> surface fluxes at grid point scale estimated from a global 21 year reanalysis of atmospheric measurements, *J. Geophys. Res.*, 115, D21307, doi:10.1029/2010JD013887, 2010.

Chimot J., Bréon F.-M., Prunet P., Vinuesa J.-F., Camy-Peyret C., Broquet G., Chevallier F., Renault E., Houweling S., Buchwitz M., Bovensmann H., Pillai D., Reuter M., Marshall J.,

Brunner D., Bergamaschi P., Ciais P., Klonecki A., LOGOFLUX – CarbonSat Earth Explorer 8 Candidate Mission – Inverse Modelling and Mission Performance Study, Final report of ESA study contract n°40010537/12/NL/CO, project led by NOVELTIS (France), NOV-7090-NT-2516, 2014.

Ciais, P., Crisp, D., Gon, H. v. d., Engelen, R., Heimann, M., Janssens-Maenhout, G., Rayner, P., and Scholze, M.: Towards a European Operational Observing System to Monitor Fossil CO<sub>2</sub> emissions - Final Report from the expert group. European Commission, Copernicus Climate Change Service, [http://www.copernicus.eu/sites/default/files/library/CO<sub>2</sub>\\_Report\\_22Oct2015.pdf](http://www.copernicus.eu/sites/default/files/library/CO2_Report_22Oct2015.pdf), 2015.

Claeyman, M. J.-L. Attie, L. El Amraoui, D. Cariolle, V.-H. Peuch, H. Teyssedre, B. Josse, P. Ricaud, S. Massart, A. Piacentini, J.-P. Cammas, N. J. Livesey, H. C. Pumphrey, and D. P. Edwards : A linear CO chemistry parameterization in a chemistry-transport model: evaluation and application to data assimilation, *Atmos. Chem. Phys.*, 10, 6097–6115, 2010.

Denier van der Gon, H. A. C., Kuenen, J. J. P., Janssens-Maenhout, G., Döring, U., Jonkers, S., and Visschedijk, A.: TNO\_CAMS high resolution European emission inventory 2000–2014 for anthropogenic CO<sub>2</sub> and future years following two different pathways, *Earth Syst. Sci. Data Discuss.*, doi:10.5194/essd-2017-124, in review, 2017.

Diamantakis, M. and A. Agustí-Panareda: A positive definite tracer mass fixer for high resolution weather and atmospheric composition forecasts, ECMWF Technical Memorandum No. 819, <https://www.ecmwf.int/sites/default/files/elibrary/2017/17914-positive-definite-tracer-mass-fixer-high-resolution-weather-and-atmospheric-composition.pdf>, December 2017.

Fountoukis, C. and Nenes, A.: ISORROPIA II: a computation-ally efficient thermodynamic equilibrium model for K<sup>+</sup>–Ca<sup>2+</sup>–Mg<sup>2+</sup>–NH<sub>4</sub><sup>+</sup>–Na<sup>+</sup>–SO<sub>4</sub><sup>2-</sup>–NO<sub>3</sub><sup>-</sup>–Cl<sup>-</sup>–H<sub>2</sub>O aerosols, *Atmos. Chem. Phys.*, 7, 4639–4659, <https://doi.org/10.5194/acp-7-4639-2007>, 2007.

Gery, M. W., Whitten, G. Z., Killus, J. P., and Dodge, M. C.: A photochemical kinetics mechanism for urban and regional scale computer modeling, *J. Geophys. Res.*, 94, 12925–12956, <https://doi.org/10.1029/JD094iD10p12925>, 1989.

Granier, C., Bessagnet, B., Bond, T., D’Angiola, A., Denier van der Gon, H., Frost, G. J., Heil, A., Kaiser, J. W., Kinne, S., Klimont, Z., Kloster, S., Lamarque, J.-F., Liousse, C., Masui, T., Meleux, F., Mieville, A., Ohara, R., Raut, J.-C., Riahi, K., Schultz, M. G., Smith, S. G., Thompson, A., van Aardenne, J., van der Werf, G. R., and van Vuuren, D. P.: Evolution of anthropogenic and biomass burning emissions of air pollutants at global and regional scales during the 1980–2010 period, *Clim. Change*, 109, 163–190, doi:10.1007/s10584-011-0154-1, 2011.

Hortal, M.: The development and testing of a new two-time level semi-Lagrangian scheme (SETTLS) in the ECMWF forecast model, *Q. J. Roy. Meteor. Soc.*, 128, 1671–1687, doi:10.1002/qj.200212858314, 2002.

Inness, A., Blechschmidt, A.-M., Bouarar, I., Chabrillat, S., Crepulja, M., Engelen, R. J., Eskes, H., Flemming, J., Gaudel, A., Hendrick, F., Huijnen, V., Jones, L., Kapsomenakis, J., Katragkou, E., Keppens, A., Langerock, B., de Mazière, M., Melas, D., Parrington, M., Peuch, V. H., Razinger, M., Richter, A., Schultz, M. G., Suttie, M., Thouret, V., Vrekoussis, M., Wagner, A., and Zerefos, C.: Data assimilation of satellite-retrieved ozone, carbon monoxide and nitrogen dioxide with ECMWF’s Composition-IFS, *Atmos. Chem. Phys.*, 15, 5275–5303, doi:10.5194/acp-15-5275-2015, 2015.

Jung, M., K. Henkel, M. Herold, and G. Churkina (2006), Exploiting synergies of global land cover products for carbon cycle modeling, *Remote Sensing of the Environment*, 101, 534–553.

Kaiser, J. W., Heil, A., Andreae, M. O., Benedetti, A., Chubarova, N., Jones, L., Morcrette, J.-J., Razinger, M., Schultz, M. G., Suttie, M., and van der Werf, G. R.: Biomass burning emissions estimated with a global fire assimilation system based on observed fire radiative power, *Biogeosciences*, 9, 527–554, doi:10.5194/bg-9-527-2012, 2012.

Koehler, M., Ahlgrimm, M., and Beljaars, A.: Unified treatment of dry convective and stratocumulus-topped boundary layers in the ecmwf model, *Q. J. Roy. Meteor. Soc.*, 137, 43–57, 2011.

Krings, T., Neininger, B., Gerilowski, K., Krautwurst, S., Buchwitz, M., Burrows, J. P., Lindemann, C., Ruhtz, T., Schüttemeyer, D., and Bovensmann, H.: Airborne remote sensing and in situ measurements of atmospheric CO<sub>2</sub> to quantify point source emissions, *Atmos. Meas. Tech.*, 11, 721-739, <https://doi.org/10.5194/amt-11-721-2018>, 2018.

Kuhlmann and Brunner, Requirements for Model Simulations Covering a Large City and a Power Plant, Deliverable 1 of ESA study SMARTCARB, contract n° 4000119599/16/NL/FF/mg, final version 7 Jun 2017. Liu, Y., Gruber, N., and Brunner, D.: Spatiotemporal patterns of the fossil-fuel CO<sub>2</sub> signal in central Europe: Results from a high-resolution atmospheric transport model, *Atmos. Chem. Phys. Discuss.*, 2017, 1-38, doi: 10.5194/acp-2017-20, 2017.

LOGOFLUX-1, Final report of CarbonSat Earth Explorer 8 Candidate Mission “LOGOFLUX 1 – Inverse Modelling and Mission Performance Study”, NOVELTIS, version 1.1, 23 July 2014

LOGOFLUX-2, Final report of CarbonSat Earth Explorer 8 Candidate Mission “LOGOFLUX 2– Flux Inversion Performance Study”, NOVELTIS, version 1.1, 12 October 2015.

Mahadevan, P., S. C. Wofsy, D. M. Matross, X. Xiao, A. L. Dunn, J. C. Lin, C. Gerbig, J. W. Munger, V. Y. Chow, and E. W. Gottlieb (2008), A satellite-based biosphere parameterization for net ecosystem CO<sub>2</sub> exchange: Vegetation Photosynthesis and Respiration Model (VPRM), *Global Biogeochem. Cycles*, 22, GB2005, doi:10.1029/2006GB002735.

Manders, A. M. M., Buitjes, P. J. H., Curier, L., Denier van der Gon, H. A. C., Hendriks, C., Jonkers, S., Kranenburg, R., Kuenen, J. J. P., Segers, A. J., Timmermans, R. M. A., Visschedijk, A. J. H., Wichink Kruit, R. J., van Pul, W. A. J., Sauter, F. J., van der Swaluw, E., Swart, D. P. J., Douros, J., Eskes, H., van Meijgaard, E., van Ulft, B., van Velthoven, P., Banzhaf, S., Mues, A. C., Stern, R., Fu, G., Lu, S., Heemink, A., van Velzen, N., and Schaap, M.: Curriculum vitae of the LOTOS–EUROS (v2.0) chemistry transport model, *Geosci. Model Dev.*, 10, 4145-4173, <https://doi.org/10.5194/gmd-10-4145-2017>, 2017.

Massart, S., Agustí-Panareda, A., Aben, I., Butz, A., Chevallier, F., Crevoisier, C., Engelen, R., Frankenberg, C., and Hasekamp, O.: Assimilation of atmospheric methane products into the MACC-II system: from SCIAMACHY to TANSO and IASI, *Atmos. Chem. Phys.*, 14, 6139–6158, doi:10.5194/acp-14-6139-2014, 2014.

Massart, S., Agustí-Panareda, A., Heymann, J., Buchwitz, M., Chevallier, F., Reuter, M., Hilker, M., and Burrows, J.: Ability of the 4D-Var analysis of the GOSAT BESD XCO<sub>2</sub> retrievals to characterize atmospheric CO<sub>2</sub> at large and synoptic scales, *Atmos. Chem. Phys.*, 16, 1653–1671, doi:10.5194/acp-16-1653-2016, 2016.

Olivier, J.G.J., G. Janssens-Maenhout, M. Muntean, J.A.H.W. Peters: Trends in global CO<sub>2</sub> emissions: 2015 Report, JRC Technical Note number: JRC98184,

[http://edgar.jrc.ec.europa.eu/news\\_docs/jrc-2015-trends-in-global-CO2-emissions-2015-report-98184.pdf](http://edgar.jrc.ec.europa.eu/news_docs/jrc-2015-trends-in-global-CO2-emissions-2015-report-98184.pdf), 2015.

Roches, A. and Fuhrer, O.: Tracer module in the COSMO model, COSMO Technical Report, available online at <http://cosmo-model.org>, 2012.

Rödenbeck, C., Bakker, D. C. E., Metzl, N., Olsen, A., Sabine, C. L. et al.: Interannual sea-air CO<sub>2</sub> flux variability from an observation-driven ocean mixed-layer scheme.

*Biogeosciences Discussions*, European Geosciences Union, 2014, 11, pp.3167-3207.  
Sandu, I., Beljaars, A., Bechtold, P., Mauritsen, T., and Balsamo, G.: Why is it so difficult to represent stably stratified conditions in numerical weather prediction (NWP) models?, *J. Adv. Modeling Earth Syst.*, 5, 1–17, doi:10.1002/jame.20013, 2013.

Skamarock, W. C., J. B. Klemp, J. Dudhia, D. O. Gill, D. M. Barker, M. G. Duda, X.-Y. Huang, W. Wang and J. G. Powers, 2008: A Description of the Advanced Research WRF Version 3, Tech. Note, NCAR/TN-475+STR, National Center for Atmos. Research, Boulder, Colorado, USA.

Spanhi, R., R. Wania, L. Need, M. van Weele, I. Pison, P. Bousquet, C. Frankenberg, P.N. Foster, F. Joos, I.C. Prentice and P. van Velthoven: Constraining global methane emissions and uptake by ecosystems, *Biogeosciences*, 8, 1643–1665, 2011.

Takahashi, T., Sutherland, S., Wanninkhof, R., Sweeney, C., Feely, R., Chipman, D., Hales, B., Friederich, G., Chavez, F., Watson, A., Bakker, D., Schuster, U., Metzl, N., Yoshikawa-Inoue, H., Ishii, M., Midorikawa, T., Nojiri, Y., Sabine, C., Olafsson, J., Arnarson, T., Tilbrook, B., Johannessen, T., Olsen, A., Bellerby, R., Körtzinger, A., Steinhoff, T., Hoppema, M., de Baar, H., Wong, C., Delille, B., and Bates, N. R.: Climatological mean and decadal changes in surface ocean pCO<sub>2</sub>, and net sea-air CO<sub>2</sub> flux over the global oceans, *Deep-Sea Res. Pt. II*, 56, 554–577, 2009.

Temperton, C., Hortal, M., and Simmons, A.: A two-time-level semi-Lagrangian global spectral model, *Q. J. Roy. Meteor. Soc.*, 127, 111–126, 2001.

Tiedtke, M.: A comprehensive mass flux scheme for cumulus parameterization in large-scale models, *Mon. Weather Rev.*, 117, 1779–1800, 1989.

Untch, A. and Hortal, M.: A finite-element scheme for the vertical discretization of the semi-Lagrangian version of the ECMWF forecast model, *Q. J. Roy. Meteor. Soc.*, 130, 1505–1530, doi:10.1256/qj.03.173, 2006.

# 11 Annex

## 11.1 Time profiles applied to emissions in the European and Berlin simulations

Table 8: Emission temporal profiles for month in year

SNAP1 category		jan	feb	mar	apr	may	jun	jul	aug	sep	oct	nov	dec
01.00	Public power stations	1.2	1.15	1.05	1	0.9	0.85	0.8	0.875	0.95	1	1.075	1.15
02.00	Commercial, institutional and residential combustion	1.7	1.5	1.3	1	0.7	0.4	0.2	0.4	0.7	1.05	1.4	1.65
34.00	Industry	1.1	1.075	1.05	1	0.95	0.9	0.93	0.95	0.97	1	1.025	1.05
05.00	Extraction and distribution of fossil fuels	1.2	1.2	1.2	0.8	0.8	0.8	0.8	0.8	0.8	1.2	1.2	1.2
06.00	Solvents	0.95	0.96	1.02	1	1.01	1.03	1.03	1.01	1.04	1.03	1.01	0.91
07.01	Road transport – gasoline	0.88	0.92	0.98	1.03	1.05	1.06	1.01	1.02	1.06	1.05	1.01	0.93
07.02	Road transport – diesel	0.88	0.92	0.98	1.03	1.05	1.06	1.01	1.02	1.06	1.05	1.01	0.93
07.03	Road transport – LNG	0.88	0.92	0.98	1.03	1.05	1.06	1.01	1.02	1.06	1.05	1.01	0.93
07.04	Road transport – evaporation	0.88	0.92	0.98	1.03	1.05	1.06	1.01	1.02	1.06	1.05	1.01	0.93
07.05	Road transport – brakewear	0.88	0.92	0.98	1.03	1.05	1.06	1.01	1.02	1.06	1.05	1.01	0.93
08.00	Non-road transport	0.88	0.92	0.98	1.03	1.05	1.06	1.01	1.02	1.06	1.05	1.01	0.93
09.00	Waste treatment	1	1	1	1	1	1	1	1	1	1	1	1
10.00	Agriculture	0.45	1.3	2.35	1.7	0.85	0.85	0.85	1	1.1	0.65	0.45	0.45



**Table 9: Emission temporal profiles for day in week**

<b>SNAP1 category</b>		<b>mon</b>	<b>Tue</b>	<b>wed</b>	<b>thu</b>	<b>fri</b>	<b>sat</b>	<b>sun</b>
01.00	Public power stations	1.06	1.06	1.06	1.06	1.06	0.85	0.85
02.00	Commercial, institutional and residential combustion	1.08	1.08	1.08	1.08	1.08	0.8	0.8
34.00	Industry	1.08	1.08	1.08	1.08	1.08	0.8	0.8
05.00	Extraction and distribution of fossil fuels	1	1	1	1	1	1	1
06.00	Solvents	1.2	1.2	1.2	1.2	1.2	0.5	0.5
07.01	Road transport – gasoline	1.02	1.06	1.08	1.1	1.14	0.81	0.79
07.02	Road transport – diesel	1.02	1.06	1.08	1.1	1.14	0.81	0.79
07.03	Road transport – LNG	1.02	1.06	1.08	1.1	1.14	0.81	0.79
07.04	Road transport – evaporation	1.02	1.06	1.08	1.1	1.14	0.81	0.79
07.05	Road transport – brakewear	1.02	1.06	1.08	1.1	1.14	0.81	0.79
08.00	Non-road transport	1	1	1	1	1	1	1
09.00	Waste treatment	1	1	1	1	1	1	1
10.00	Agriculture	1	1	1	1	1	1	1

**Table 10: Emission temporal profiles for hour in day (first 12 hours)**

<b>SNAP1 category</b>		<b>1</b>	<b>2</b>	<b>3</b>	<b>4</b>	<b>5</b>	<b>6</b>	<b>7</b>	<b>8</b>	<b>9</b>	<b>10</b>	<b>11</b>	<b>12</b>
01.00	Public power stations	0.79	0.72	0.72	0.71	0.74	0.8	0.92	1.08	1.19	1.22	1.21	1.21
02.00	Commercial, institutional and residential combustion	0.38	0.36	0.36	0.36	0.37	0.5	1.19	1.53	1.57	1.56	1.35	1.16
34.00	Industry	0.75	0.75	0.78	0.82	0.88	0.95	1.02	1.09	1.16	1.22	1.28	1.3
05.00	Extraction and distribution of fossil fuels	1	1	1	1	1	1	1	1	1	1	1	1
06.00	Solvents	0.5	0.35	0.2	0.1	0.1	0.2	0.75	1.25	1.4	1.5	1.5	1.5
07.01	Road transport – gasoline	0.19	0.09	0.06	0.05	0.09	0.22	0.86	1.84	1.86	1.41	1.24	1.2
07.02	Road transport – diesel	0.19	0.09	0.06	0.05	0.09	0.22	0.86	1.84	1.86	1.41	1.24	1.2
07.03	Road transport – LNG	0.19	0.09	0.06	0.05	0.09	0.22	0.86	1.84	1.86	1.41	1.24	1.2
07.04	Road transport – evaporation	0.19	0.09	0.06	0.05	0.09	0.22	0.86	1.84	1.86	1.41	1.24	1.2
07.05	Road transport – brakewear	0.19	0.09	0.06	0.05	0.09	0.22	0.86	1.84	1.86	1.41	1.24	1.2
08.00	Non-road transport	1	1	1	1	1	1	1	1	1	1	1	1
09.00	Waste treatment	1	1	1	1	1	1	1	1	1	1	1	1
10.00	Agriculture	0.6	0.6	0.6	0.6	0.6	0.65	0.75	0.9	1.1	1.35	1.45	1.6

Table 11: Emission temporal profiles for hour in day (last 12 hours)

SNAP1 category		13	14	15	16	17	18	19	20	21	22	23	24
01.00	Public power stations	1.17	1.15	1.14	1.13	1.1	1.07	1.04	1.02	1.02	1.01	0.96	0.88
02.00	Commercial, institutional and residential combustion	1.07	1.06	1	0.98	0.99	1.12	1.41	1.52	1.39	1.35	1	0.42
34.00	Industry	1.22	1.24	1.25	1.16	1.08	1.01	0.95	0.9	0.85	0.81	0.78	0.75
05.00	Extraction and distribution of fossil fuels	1	1	1	1	1	1	1	1	1	1	1	1
06.00	Solvents	1.5	1.5	1.5	1.5	1.5	1.4	1.25	1.1	1	0.9	0.8	0.7
07.01	Road transport – gasoline	1.32	1.44	1.45	1.59	2.03	2.08	1.51	1.06	0.74	0.62	0.61	0.44
07.02	Road transport – diesel	1.32	1.44	1.45	1.59	2.03	2.08	1.51	1.06	0.74	0.62	0.61	0.44
07.03	Road transport – LNG	1.32	1.44	1.45	1.59	2.03	2.08	1.51	1.06	0.74	0.62	0.61	0.44
07.04	Road transport – evaporation	1.32	1.44	1.45	1.59	2.03	2.08	1.51	1.06	0.74	0.62	0.61	0.44
07.05	Road transport – brakewear	1.32	1.44	1.45	1.59	2.03	2.08	1.51	1.06	0.74	0.62	0.61	0.44
08.00	Non-road transport	1	1	1	1	1	1	1	1	1	1	1	1
09.00	Waste treatment	1	1	1	1	1	1	1	1	1	1	1	1
10.00	Agriculture	1.65	1.75	1.7	1.55	1.35	1.1	0.9	0.75	0.65	0.6	0.6	0.6

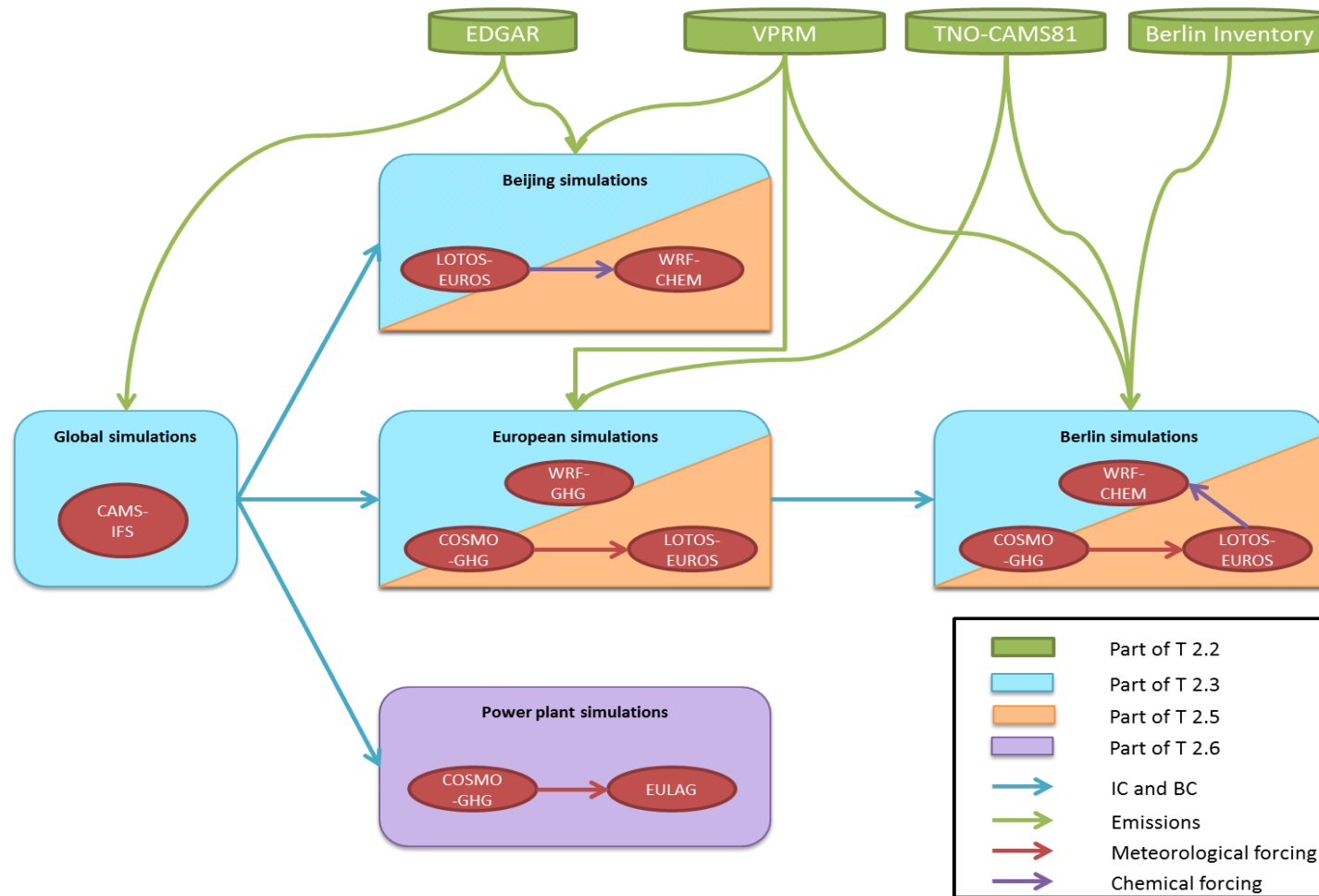
## 11.2 Vertical profiles applied to emissions in the European and Berlin simulations

Table 12: Vertical profiles as in Bieser et al., 2011

SNAP1 category		20m	92m	184m	324m	522m	781m	1106m
01.00	Public power stations	0	0	0.0025	0.51	0.453	0.0325	0.002
02.00	Commercial, institutional and residential combustion	1	0	0	0	0	0	0
34.00	Industry	0.06	0.16	0.75	0.03	0	0	0
05.00	Extraction and distribution of fossil fuels	0.02	0.08	0.6	0.3	0	0	0
06.00	Solvents	1	0	0	0	0	0	0
07.01	Road transport – gasoline	1	0	0	0	0	0	0
07.02	Road transport – diesel	1	0	0	0	0	0	0
07.03	Road transport – LNG	1	0	0	0	0	0	0
07.04	Road transport – evaporation	1	0	0	0	0	0	0
07.05	Road transport – brakewear	1	0	0	0	0	0	0
08.00	Non-road transport	1	0	0	0	0	0	0
09.00	Waste treatment	0	0	0.41	0.57	0.02	0	0
10.00	Agriculture	1	0	0	0	0	0	0

### 11.3 Schematic of the interdependence of the simulations

Figure 9: Schematic of the interdependence of the different simulations and models



## 11.4 Summary of all the simulations

Table 13: List of simulations

ID	Responsible	Model	Resolution	Meteo.	Emissions	Driving meteo.	IC/BC Meteo.	IC/BC Tracers	Tracers
GLOB-2015-TIER1	ECMWF	C-IFS	approx. 9 km	2015	EDGAR 4.2FT2010	online	daily reinitialization from op. anal.	-	CO <sub>2</sub> , CO
GLOB-2015-TIER2	ECMWF	C-IFS, Ensemble	open	2015	EDGAR 4.3.2FT	online	daily reinitialization from op. anal.	-	CO <sub>2</sub> , CO
GLOB-2030-TIER2	ECMWF	C-IFS, Ensemble	open	2015	EDGAR 4.3.2FT_CIRCE	online	daily reinitialization from op. anal.	-	CO <sub>2</sub> , CO
EU-2015	Empa	COSMO-GHG	approx. 5 km	2015	TNO/CAMS81	online	daily reinitialization from op. anal.	GLOB-2015-TIER2	CO <sub>2</sub> , CO (APO, 14C, COsim)
	Empa	COSMO-GHG	approx. 5 km	2015	EDGAR 4.3.2FT	online	daily reinitialization from op. anal.	GLOB-2015-TIER2	CO <sub>2</sub> , CO
	MPG	WRF-GHG	approx. 5 km	2015	TNO/CAMS81	online	daily reinitialization from op. anal.	GLOB-2015-TIER2	CO <sub>2</sub> , CO (APO, 14C)
	TNO	LOTOS-EUROS	approx. 5 km	2015	TNO/CAMS81	COSMO-GHG	-	GLOB-2015-TIER2, CAMS	CO <sub>2</sub> , CO, NO <sub>x</sub> , aerosols
EU-2030-BAU	Empa	COSMO-GHG	approx. 5 km	2015	TNO/CAMS81-BAU	online	daily reinitialization from GLOB-2030-TIER2	GLOB-2030-TIER2	CO <sub>2</sub> , CO
	MPG	WRF-GHG	approx. 5 km	2015	TNO/CAMS81-BAU	online	daily reinitialization from GLOB-2030-TIER2	GLOB-2030-TIER2	CO <sub>2</sub> , CO
	TNO	LOTOS-EUROS	approx. 5 km	2015	TNO/CAMS81-BAU	COSMO-GHG	-	GLOB-2030-TIER2, CAMS	CO <sub>2</sub> , CO, NO <sub>x</sub> , aerosols

CO<sub>2</sub> HUMAN EMISSIONS 2018

EU-2030-CC	EMPA	COSMO-GHG	approx. 5 km	2015	TNO/CAMS81-CC	online	daily reinitialization from GLOB-2030-TIER2	GLOB-2030-TIER2	CO <sub>2</sub> , CO
	MPG	WRF-GHG	approx. 5 km	2015	TNO/CAMS81-CC	online	GLOB-2030-TIER2	GLOB-2030-TIER2	CO <sub>2</sub> , CO
	TNO	LOTOS-EUROS	approx. 5 km	2015	TNO/CAMS81-CC	COSMO-GHG	-	GLOB-2030-TIER2, CAMS	CO <sub>2</sub> , CO, NO <sub>x</sub> , aerosols
Berlin-2015	Empa	COSMO-GHG	approx. 1 km	2015	TNO/CAMS81-hires	online	COSMO EU-2015	EU-2015	CO <sub>2</sub> , CO
Berlin-2015-summer	TNO	LOTOS-EUROS	approx. 2 km	June 26 - July 14 2015	TNO/CAMS81-hires	COSMO-GHG	-	EU-2015	CO <sub>2</sub> , CO, NO <sub>x</sub> , aerosols
	SRON	WRF-CHEM	approx. 1 km	June 26 - July 14 2015	TNO/CAMS81-hires	online	WRF EU-2015	EU-2015	CO <sub>2</sub>
Berlin-2015-winter	TNO	LOTOS-EUROS	approx. 2 km	Feb 1 - 20 2015	TNO/CAMS81-hires	COSMO-GHG	-	EU-2015	CO <sub>2</sub> , CO, NO <sub>x</sub> , aerosols
	SRON	WRF-CHEM	approx. 1 km	Feb 1 - 20 2015	TNO/CAMS81-hires	online	WRF EU-2015	EU-2015	CO <sub>2</sub>
Beijing-2013-summer	TNO	LOTOS-EUROS		Jun 16 - 29 2013	EDGAR 4.3.2FT			CAMS	CO <sub>2</sub> , CO, NO <sub>x</sub> , aerosols
	SRON	WRF-CHEM	approx. 1 km	Jun 16 - 29 2013	EDGAR 4.3.2FT	online		CAMS	CO <sub>2</sub>
Beijing-2013-winter	TNO	LOTOS-EUROS		Jan 11 - 24 2013	EDGAR 4.3.2FT			CAMS	CO <sub>2</sub> , CO, NO <sub>x</sub> , aerosols
	SRON	WRF-CHEM	approx. 1 km	Jan 11 - 24 2013	EDGAR 4.3.2FT	online		CAMS	CO <sub>2</sub>
PowerPlant-case1	SPASCIA	EULAG	approx. 100 m	August 2012		COSMO-GHG			

CO<sub>2</sub> HUMAN EMISSIONS 2018

	Empa	COSMO-GHG	approx. 1 km	August 2012		online			
--	------	-----------	--------------	-------------	--	--------	--	--	--

## Document History

Version	Author(s)	Date	Changes
1.0	Haussaire, Brunner (Empa)	08/03/2018	First draft
2.0	Haussaire, Brunner (Empa)	27/03/2018	Post review version

## Internal Review History

Internal Reviewers	Date	Comments
Frederic Chevalier (CEA)	23/03/2018	Approved with comments
Rosemary Munro (EUMETSAT)	23/03/2018	Approved with comments

## Estimated Effort Contribution per Partner

Partner	Effort
Empa	2
ECMWF	0.1
SPASCIA	0.1
TNO	0.1
JRC	0.1
SRON	0.1
<b>Total</b>	<b>2.5</b>

This publication reflects the views only of the author, and the Commission cannot be held responsible for any use which may be made of the information contained therein.

